J Arid Land (2023) 15(3): 231–252
https://doi.org/10.1007/s40333-023-0053-0

Science Press Springer-Verlag

Spatial-temporal changes and driving factors of eco-environmental quality in the Three-North region of China

LONG Yi[1,2,3], JIANG Fugen[1,2,3], DENG Muli[1,2,3], WANG Tianhong[1,2,3], SUN Hua[1,2,3*]

[1] Research Center of Forestry Remote Sensing & Information Engineering, Central South University of Forestry and Technology, Changsha 410004, China;
[2] Key Laboratory of Forestry Remote Sensing Based Big Data & Ecological Security for Hunan Province, Changsha 410004, China;
[3] Key Laboratory of National Forestry & Grassland Administration on Forest Resources Management and Monitoring in Southern Area, Changsha 410004, China

Abstract: Eco-environmental quality is a measure of the suitability of the ecological environment for human survival and socioeconomic development. Understanding the spatial-temporal distribution and variation trend of eco-environmental quality is essential for environmental protection and ecological balance. The remote sensing ecological index (RSEI) can quickly and objectively quantify eco-environmental quality and has been extensively utilized in regional ecological environment assessment. In this paper, Moderate Resolution Imaging Spectroradiometer (MODIS) images during the growing period (July–September) from 2000 to 2020 were obtained from the Google Earth Engine (GEE) platform to calculate the RSEI in the three northern regions of China (the Three-North region). The Theil-Sen median trend method combined with the Mann-Kendall test was used to analyze the spatial-temporal variation trend of eco-environmental quality, and the Hurst exponent and the Theil-Sen median trend were superimposed to predict the future evolution trend of eco-environmental quality. In addition, ten variables from two categories of natural and anthropogenic factors were analyzed to determine the drivers of the spatial differentiation of eco-environmental quality by the geographical detector. The results showed that from 2000 to 2020, the RSEI in the Three-North region exhibited obvious regional characteristics: the RSEI values in Northwest China were generally between 0.2 and 0.4; the RSEI values in North China gradually increased from north to south, ranging from 0.2 to 0.8; and the RSEI values in Northeast China were mostly above 0.6. The average RSEI value in the Three-North region increased at an average growth rate of 0.0016/a, showing the spatial distribution characteristics of overall improvement and local degradation in eco-environmental quality, of which the areas with improved, basically stable and degraded eco-environmental quality accounted for 65.39%, 26.82% and 7.79% of the total study area, respectively. The Hurst exponent of the RSEI ranged from 0.20 to 0.76 and the future trend of eco-environmental quality was generally consistent with the trend over the past 21 years. However, the areas exhibiting an improvement trend in eco-environmental quality mainly had weak persistence, and there was a possibility of degradation in eco-environmental quality without strengthening ecological protection. Average relative humidity, accumulated precipitation and land use type were the dominant factors driving the spatial distribution of eco-environmental quality in the Three-North region, and two-factor interaction also had a greater influence on eco-environmental quality than single factors. The explanatory power of meteorological factors on the spatial distribution of eco-environmental quality was stronger than that of topographic factors. The effect of anthropogenic factors (such as population density and land use type) on eco-environmental quality gradually increased over time. This study can

*Corresponding author: SUN Hua (E-mail: sunhua@csuft.edu.cn)
Received 2022-07-07; revised 2022-11-21; accepted 2022-11-27

serve as a reference to protect the ecological environment in arid and semi-arid regions.

Keywords: eco-environmental quality; remote sensing ecological index; Google Earth Engine; Hurst exponent; geographical detector; Three-North region of China

Citation: LONG Yi, JIANG Fugen, DENG Muli, WANG Tianhong, SUN Hua. 2023. Spatial-temporal changes and driving factors of eco-environmental quality in the Three-North region of China. Journal of Arid Land, 15(3): 231–252. https://doi.org/10.1007/s40333-023-0053-0

1 Introduction

As climate change and human activities intensify, ecological environment problems have gradually threatened regional ecological security and socioeconomic sustainable development (Liao et al., 2020). Together, the three northern regions of China (i.e., the Three-North region), including Northwest China, North China and Northeast China, constitute one of the most crucial natural resource reserves in China and form an important ecological barrier. With nearly 280,000 km^2 of suitable forestland (accounting for nearly two-thirds of the total suitable forestland in the country), the Three-North region has great potential to increase forest resources and is the key area for forestland and grassland construction and carbon sinks in China (Zhang et al., 2021a). However, the natural environment in the Three-North region is fragile and variable, and most of the region is located in arid and semi-arid climate zones (Zhang et al., 2021a). In 1978, the Three-North Shelterbelt Program, which covers 13 provinces, autonomous regions and municipalities in China, was launched to alleviate soil erosion and wind-blown sand hazards in the Three-North region (Duan et al., 2011; Deng et al., 2019). Since the implementation of the program, the ecological status and economic benefits of the project area have been greatly improved, playing an important role in maintaining national ecological security and promoting socioeconomic sustainable development (Cao et al., 2020). In recent years, to enhance the carbon sink potential of forestland and grassland in the Three-North region and achieve carbon peaking and carbon neutrality, the Chinese government has intensified efforts to protect and restore important ecosystems through the Three-North Shelterbelt Program (Lu et al., 2018); therefore, eco-environmental quality in the project area has been continuously improved. Eco-environmental quality is the comprehensive performance of ecosystem elements, structure and functional characteristics. Superior eco-environmental quality fundamentally guarantees human survival and is the physical prerequisite for socioeconomic progress (Jiang et al., 2021). Mastering the spatial-temporal distribution and variation trend of eco-environmental quality is helpful for ecological protection, environmental restoration and policy formulation in the Three-North region. It is important to comprehensively promote the carbon sink capacity of the ecosystem in the project area and to achieve both the 'double carbon' goal and sustainable development (Lu et al., 2018).

The traditional evaluation of eco-environmental quality has primarily been based on the statistical yearbooks (Shan et al., 2019; Wang et al, 2019). Annual data were recorded systematically and continuously; however, basic data points regarding vegetation, soil and hydrology over large areas on monthly or quarterly scales have not been collected. Annual data are limited in their usefulness for the dynamic monitoring of eco-environmental quality over short intervals (Zhong et al., 2020). Remote sensing technology has the advantages of fast, real-time and widespread coverage. It also offers technical support for the monitoring and evaluation of eco-environmental quality (Zheng et al., 2020; Zhou and Liu, 2022). Monitoring indices constructed using remote sensing technology have become the primary means of the monitoring and evaluation of regional eco-environmental quality. For example, the normalized difference vegetation index (NDVI) has been widely used to evaluate vegetation growth and phenology (Erasmi et al., 2021; Zhang et al., 2021b), the water index has been applied to evaluate drought status or habitat suitability (Mishra and Pant, 2020; Al-Quraishi et al., 2021), and the land surface temperature (LST) has been used to evaluate the urban heat island effect (Lee and Park, 2020;

Arshad et al., 2022). The ecological environment is composed of complex ecosystems and is affected by multiple factors; therefore, a remote sensing evaluation method based on a single monitoring index cannot comprehensively capture the systematic changes in eco-environmental quality (Wen et al., 2019; Zhou and Liu, 2022). The Ministry of Ecology and Environment of the People's Republic of China proposed the ecological index (EI) to evaluate the regional eco-environmental quality in China from the five aspects of biology, vegetation, hydrology, land and pollution (Shan et al., 2019; Zhou and Liu, 2022). However, the EI can only provide a general overview of the ecological situation of a region, rather than a detailed description of the local distribution of various environmental conditions in the region. Based on the EI and remote sensing data, researchers constructed the remote sensing ecological index (RSEI) using principal component transformation to couple measures of greenness, humidity, dryness and heat (Hu and Xu, 2018; Xu et al., 2019). The RSEI can overcome the spatial visualization difficulties of the EI and reduce the impact of anthropogenic factors in the evaluation process (Hu and Xu, 2018; Xu et al., 2018). It has been widely used for monitoring eco-environmental quality in cities (Wen et al., 2019; Sajjad et al., 2021), lakes (Xiong et al., 2021; Yuan et al., 2021) and other regions.

The dynamic analysis of time series remote sensing images is important for identifying the changes and internal laws of eco-environmental quality. The existing research methods for long-term sequences are numerous and have been used frequently, providing reference for their application to the spatial-temporal analysis of eco-environmental quality (Sun et al., 2020; Li et al., 2021a; Li et al., 2021b; Xu et al., 2021; Jiang et al., 2022). The linear trend analysis method is commonly used to describe the trend and change of time series data by obtaining the slope to estimate the magnitude of the variation trend through regression analysis (Duan et al., 2011; Deng et al., 2019; Xu et al., 2021). However, this method has limited stability and is sensitive to anomalous data. The Theil-Sen median is a nonparametric statistical trend estimator that is often combined with the Mann-Kendall (MK) test for the trend analysis of long-term sequence data (Li et al., 2021a; Zhang et al., 2021b; Jiang et al., 2022). Compared with the linear trend analysis method, the Theil-Sen median trend method combined with the MK test has high calculation efficiency and robustness to error, which effectively reduces the influence of data outliers and improves the accuracy of test results. In addition, the Hurst exponent can be calculated to predict the future trend of time series data (Li et al., 2021a; Li et al., 2021b; Rivas-Tabares et al., 2021), and the coefficient of variation (Li et al., 2021b; Zhang et al., 2021b), Moran index (Xiong et al., 2021) and change vector analysis (Xu et al., 2019; Sun et al., 2020) can be effectively used to understand the spatial evolutionary characteristics of vegetation.

Natural factors control the evolution of the ecosystem environment, while human activities can have a considerable impact on the ecological environment of a local area. Therefore, a combination of natural factors (temperature, precipitation, etc.) and anthropogenic factors (population, land use, etc.) may contribute to the changes in eco-environmental quality (Gao et al., 2020; Sun et al., 2020). Correlation and partial correlation analyses are commonly used to determine the relationship between drivers and response variables (Hu et al., 2021; Liu et al., 2021). Correlation analysis can assess the influence or association between two factors without considering the influence of other factors (Hu et al., 2021). Partial correlation analysis can identify the interaction between specific variables after controlling the influence of other factors (Liu et al., 2021). Correlation and partial correlation analyses are limited in their ability to quantify the coupling effects of multiple factors; however, the geographical detector can overcome this problem. The geographical detector, which is based on the factor force measurement index, can detect spatial differentiation by combining spatial superposition techniques and set theory to reveal the driving forces behind the differentiation mechanism (Wang et al., 2010; Wang and Hu, 2012).

Optical data, such as Moderate Resolution Imaging Spectroradiometer (MODIS) and Landsat images, are commonly used data sources for constructing the RSEI (Shan et al., 2019; Wen et al., 2019; Liao et al., 2020; Zheng et al., 2020). Due to the influence of weather, topography and other conditions, it is difficult to obtain cloudless Landsat images of a large area in the same period (Ji

et al., 2020). MODIS data have high spatial resolution and represent a complete time series, but they require excessive data preprocessing and index calculation processes when applied on large regional scales (Xu et al., 2019; Zheng et al., 2020). Google Earth Engine (GEE), a remote sensing cloud platform, contains massive numbers of historical images and geographic databases and has overcome the problems of low efficiencies of local downloading, storage and preprocessing (Gorelick et al., 2017). GEE has been applied extensively for large-scale regional data fusion (Nietupski et al., 2021), crop yield estimation (Adrian et al., 2021; Venkatappa et al., 2021) and land cover dynamic analysis (Floreano and de Moraes, 2021).

In this study, GEE was used to obtain and preprocess MODIS images during the growing period (July–September) from 2000 to 2020 to calculate the RSEI for the dynamic monitoring and evaluation of eco-environmental quality in the Three-North region. The Theil-Sen median trend method combined with the MK test was used to analyze the variation trend of eco-environmental quality in the Three-North region during the study period, and the Hurst exponent and the Theil-Sen median trend were superimposed to predict the future trend of eco-environmental quality. In addition, the main drivers influencing the spatial distribution of eco-environmental quality were identified using a geographical detector to serve as a reference for securing the ecological environment in the Three-North region.

2 Materials and methods

2.1 Study area

The study area is the Three-North region (i.e., the three northern regions of China), located between 31°31′–53°34′N and 73°26′–135°06′E (Fig. 1). It includes Northwest China, North China and Northeast China, covering 13 provinces, autonomous regions and municipalities, with a total area of approximately 5,470,000 km^2. The Three-North region encompasses vast deserts, sandy lands and the Gobi, most of which are located in arid and semi-arid climate zones. The natural environment is fragile in this region. The western part is dominated by desert lands, while the eastern part is mainly covered by forestlands and grasslands. Since the implementation of the Three-North Shelterbelt Program, a total afforestation and preservation area of 301,400 km^2 has been completed in the project area (Ji et al., 2022). Over the past 40 a, the forest coverage has increased from 5.05% to 13.57%, significantly improving the ecological conditions (Li and Feng, 2021).

2.2 Data sources and processing

The remote sensing data used to calculate the RSEI include the MOD09A1 V6 and MOD11A2 V6 datasets. MOD09A1 V6 contains the surface reflectance data from the Terra MODIS sensor with a spatial resolution of 0.5 km, which is corrected for atmospheric conditions (Xu et al., 2019). MOD11A2 V6 contains the surface temperature data with a spatial resolution of 1.0 km. To reduce the interference caused by the difference in image acquisition time, we obtained both datasets (MOD09A1 V6 and MOD11A2 V6) for the growing period (July–September) from 2000 to 2020 on the GEE platform. In addition, we declouded the surface reflectance data using the quality assessment band to improve the image quality under cloud interference (Zheng and Zhu, 2017) and synthesized using the median value to stabilize the MODIS images for subsequent analysis.

Changes in ecosystems are influenced by a combination of natural factors and human activities (Jiang et al., 2021). Temperature, precipitation and other important meteorological factors have multiple impacts on ecosystems (Yuan et al., 2021). Topographic factors, as important environmental factors, can indirectly affect the growth and distribution of vegetation by influencing climate and soil (Zhang et al., 2021b). Population and socioeconomic development are important anthropogenic factors, and land use type and soil health can reflect the state of the ecological environment (Yuan et al., 2021). To explore the drivers of the spatial differentiation in eco-environmental quality in the study area, we examined ten drivers from two categories of

natural and anthropogenic factors. The natural factors included meteorological factors (cumulative precipitation, average temperature, average relative humidity and potential evapotranspiration) and topographic factors (elevation, slope and aspect). To obtain meteorological data for the corresponding time periods, we summarized the monthly average

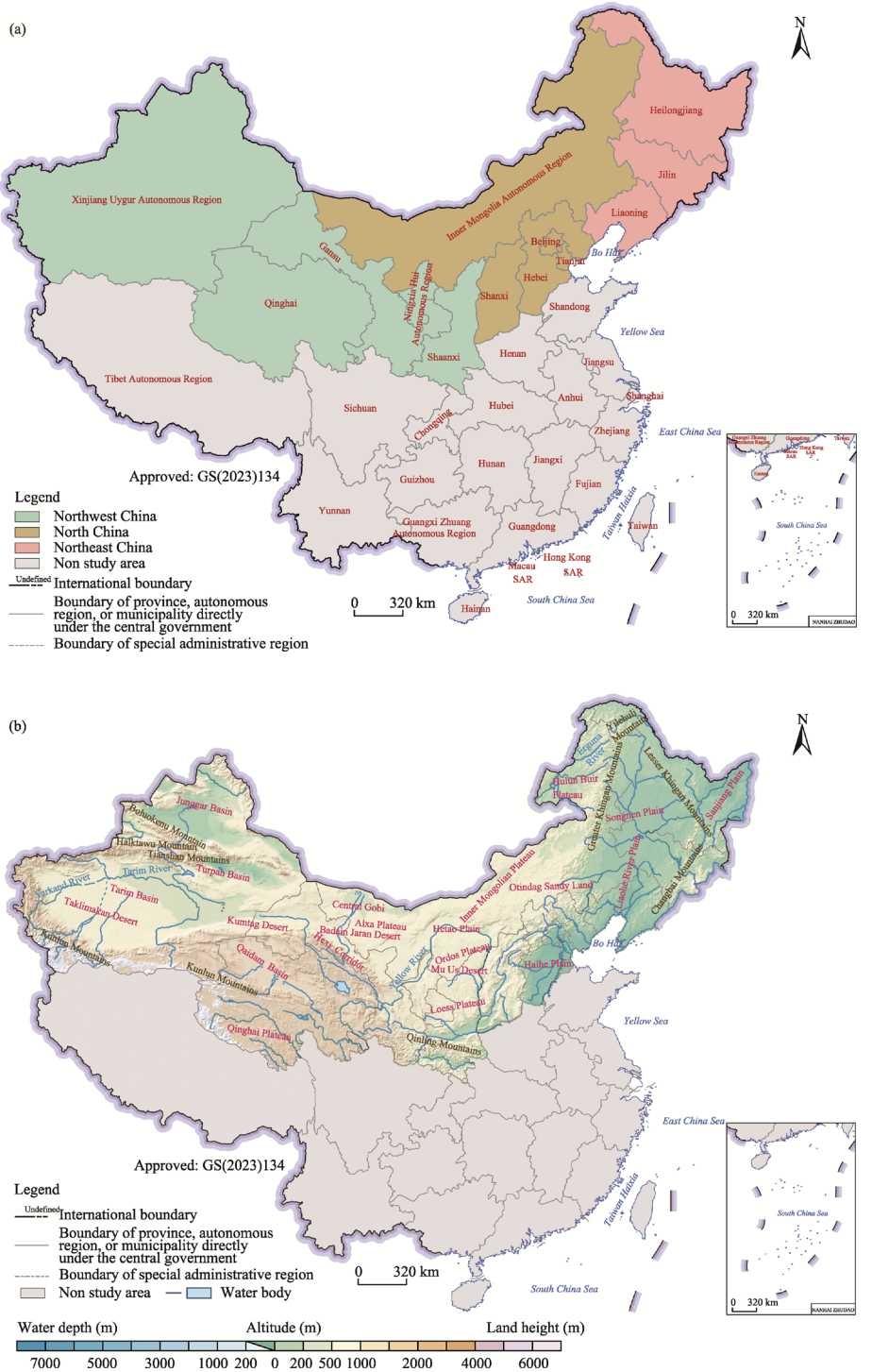

Fig. 1 Location of the study area (Three-North region) in China (a) and topography of the study area (b). The Three-North region includes Northwest China, North China and Northeast China, covering 13 provinces, autonomous regions and municipalities. SAR, special administrative region.

temperature, monthly average relative humidity and monthly potential evapotranspiration data from July to September by the mean values, and calculated the monthly cumulative precipitation data by the total amount. Anthropogenic factors included socioeconomic factors (nighttime-light and population density) and human disturbance factor (land use type). The land use type data were classified using a two-level classification system: the first level was divided into six types according to land resource and its use attribute; and the second level was divided into 25 types according to the natural attribute of land resource (Liu et al., 2010). The six types in the first level classification were used for analysis in this study, which included cultivated land, forestland, grassland, water bodies, construction land and unused land. More detailed information about these data is shown in Table 1.

Table 1 Detailed description of the data used in the study

Function	Data name	Spatial resolution	Time resolution	Time span	Source
RSEI calculation	MOD09A1 V6	0.5 km	8 d	2000–2020 (growing period)	GEE (https://developers.google.com)
	MOD11A2 V6	1.0 km	8 d		
Factor response analysis	Cumulative precipitation	1.0 km	Monthly	2000, 2005, 2010, 2015 and 2020 (growing period)	National Earth System Science Data Center and the National Science & Technology Infra-structure of China (http://www.geodata.cn)
	Average temperature	1.0 km	Monthly		
	Average relative humidity	1.0 km	Monthly		
	Potential evapotranspiration	1.0 km	Monthly		
	Elevation	1.0 km		2000	A Big Earth Data Platform for Three Poles (http://poles.tpdc.ac.cn/)
	Slope	1.0 km		2000	
	Aspect	1.0 km		2000	
	Nighttime-light	1.0 km	Annual	2000, 2005, 2010, 2015 and 2020	A Big Earth Data Platform for Three Poles (http://poles.tpdc.ac.cn/)
	Population density	1.0 km	Annual	2000, 2005, 2010, 2015 and 2020	WorldPop (https://www.worldpop.org)
	Land use type	1.0 km	Quinquennial	2000, 2005, 2010, 2015 and 2020	Resource and Environment Science and Data Center of the Chinese Academy of Sciences (https://www.resdc.cn)

Note: RSEI, remote sensing ecological index; GEE, Google Earth Engine. Growing period refers to months from July to September.

2.3 Methods

2.3.1 RSEI construction

The RSEI can assess eco-environmental quality by greenness, wetness, dryness and heat (Hu and Xu, 2018). In this study, the NDVI was used as the greenness indicator; the humidity component (Wet) obtained through the tasseled cap transformation was used as the wetness indicator (Xu et al., 2021); the normalized difference built-up and soil index (NDBSI), i.e., the mean of the soil index (SI) and index-based built-up index (IBI), was used as the dryness indicator; and the LST was used as the heat indicator.

On the GEE platform, the NDVI, Wet and NDBSI parameters were extracted using the processed surface reflectance data of MODIS images and resampled to a spatial resolution of 1.0 km to maintain consistency between different data sources. The calculation formulas of each index are as follows:

$$\mathrm{NDVI}=\frac{\rho_2-\rho_1}{\rho_2+\rho_1}, \tag{1}$$

$$\mathrm{Wet}=0.3279\rho_1+0.3406\rho_2+0.1509\rho_3+0.1973\rho_4-0.7112\rho_6-0.4572\rho_7, \tag{2}$$

$$\mathrm{SI}=\frac{(\rho_6+\rho_1)-(\rho_2+\rho_3)}{(\rho_6+\rho_1)+(\rho_2+\rho_3)}, \tag{3}$$

$$\mathrm{IBI}=\frac{\dfrac{2\rho_6}{\rho_6+\rho_2}-\left(\dfrac{\rho_2}{\rho_2+\rho_1}+\dfrac{\rho_4}{\rho_4+\rho_6}\right)}{\dfrac{2\rho_6}{\rho_6+\rho_2}+\left(\dfrac{\rho_2}{\rho_2+\rho_1}+\dfrac{\rho_4}{\rho_4+\rho_6}\right)}, \tag{4}$$

$$\mathrm{NDBSI}=\frac{\mathrm{SI}+\mathrm{IBI}}{2}, \tag{5}$$

where NDVI is the normalized difference vegetation index; Wet is the humidity component; ρ_1, ρ_2, ρ_3, ρ_4, ρ_6 and ρ_7 are the reflectance values of the red, near-infrared 1, blue, green, short wavelength infrared 1 and short wavelength infrared 2 bands of MOD09A1, respectively; SI is the soil index; IBI is the index-based built-up index; and NDBSI is the normalized difference built-up and soil index.

The daytime surface temperature data of MOD11A2 V6 were synthesized to obtain the LST. All indicators were standardized to eliminate the influence of the dimension between different indicators. In addition, water bodies were masked using the JRC Yearly Water Classification History dataset (Pekel et al., 2016) provided by the GEE platform (Source: EC JRC/Google), and the union of different years of water bodies within the study area was masked in the spatiotemporal analysis. Principal component analysis (PCA) was used to integrate the four indicators (Hong et al., 2020), and the first principal component was defined as the RSEI_0. The RSEI_0 was then standardized to obtain the RSEI to facilitate the measurement and comparison of the four indicators, as follows:

$$\mathrm{RSEI}_0=f\left(\mathrm{NDVI},\mathrm{Wet},\mathrm{NDBSI},\mathrm{LST}\right), \tag{6}$$

$$\mathrm{RSEI}=\frac{\mathrm{RSEI}_0-\mathrm{RSEI}_{0\min}}{\mathrm{RSEI}_{0\max}-\mathrm{RSEI}_{0\min}}, \tag{7}$$

where RSEI_0 is the first principal component of the four indicators; LST is the land surface temperature (K); RSEI is the remote sensing ecological index; $\mathrm{RSEI}_{0\min}$ is the minimum value of the RSEI_0; and $\mathrm{RSEI}_{0\max}$ is the maximum value of the RSEI_0.

The RSEI value is between 0.0 and 1.0. The closer the value is to 1.0, the better the quality of the ecological environment; and the closer the value is to 0.0, the worse the quality of the ecological environment. The RSEI values in the study were divided into five intervals (0.0–0.2, 0.2–0.4, 0.4–0.6, 0.6–0.8 and 0.8–1.0), corresponding to the five grades of eco-environmental quality: poor, fair, moderate, good and excellent, respectively.

2.3.2 Trend analysis

The Theil-Sen median trend method combined with the MK test was used to analyze the variation trend of eco-environmental quality in the Three-North region during the study period, and the Hurst exponent and the Theil-Sen median trend were superimposed to predict the future trend of eco-environmental quality.

(1) Trend analysis based on the Theil-Sen median trend method and MK test

As a robust method of trend calculation, the Theil-Sen median trend method is often used in conjunction with the MK test to detect the variation trend of long-term sequence data (Li et al., 2021a; Jiang et al., 2022). The calculation formula of the Theil-Sen median (β) is as follows:

$$\beta=\mathrm{median}\left(\frac{\mathrm{RSEI}_j-\mathrm{RSEI}_i}{j-i}\right)\ (2000\le i<j\le 2020), \tag{8}$$

where i and j represent the RSEI time series (i.e., 21 a from 2000 to 2020); and RSEI_i and RSEI_j represent the RSEI values of years i and j, respectively.

Referring to the classification standard of Jiang et al. (2015), we divided the variation trend of eco-environmental quality into three types based on the Theil-Sen median (β): β>0.0005 indicating an improved trend of eco-environmental quality; –0.0005≤β≤0.0005 indicating a stable trend of eco-environmental quality; and β< –0.0005 indicating a degraded trend of eco-environmental quality. The MK method used the Z statistic for the significance test. Based on a significance level of α, when $|Z|>Z_{1-\alpha/2}$, the trend of the time series is considered significant; otherwise, it is considered nonsignificant. Referring to Li et al. (2021b), the value of α was taken as 0.05 in this study, which indicated that the trend is judged to be significant at a confidence level of 95%. When α equals to 0.05, the Z-score corresponding to the cumulative probability of $1–\alpha/2$ is queried through the standard normal distribution table as 1.96 (Kutner et al., 2004). That is, the value of $Z_{1-\alpha/2}$ was 1.96 in this study. Combining the Theil-Sen median and MK test results, we divided the variation trend of eco-environmental quality into five categories. The specific classification standard is shown in Table 2.

Table 2 Classification standard for the trend analysis of eco-environmental quality based on the Theil-Sen median (β) and Mann-Kendall (MK) test results

Classification standard	Variation trend of eco-environmental quality
β< –0.0005 and $\|Z\|$>1.96	Significant degradation
β< –0.0005 and $\|Z\|$≤1.96	Slight degradation
–0.0005≤β≤0.0005	Basically stable
β>0.0005 and $\|Z\|$≤1.96	Slight improvement
β>0.0005 and $\|Z\|$>1.96	Significant improvement

Note: The MK method used the Z statistic for the significance test.

(2) Hurst exponent

The Hurst exponent reflects the autocorrelation of time series and can effectively predict future development trend (Li et al., 2021b; Rivas-Tabares et al., 2021). The calculation procedure is shown as follows.

Given a time sequence RSEI(t) (where t=1, 2, …, n), the following equations can be obtained for any positive integer (τ≥1, where τ is the integer).

$$\text{Mean sequence: } \langle \text{RSEI} \rangle_\tau = \frac{1}{\tau}\sum_{t=1}^{\tau} \text{RSEI}(t) \quad (\tau = 1,\ 2,\ \ldots,\ n). \tag{9}$$

$$\text{Accumulated deviation: } X(t,\tau) = \sum_{t=1}^{\tau} (\text{RSEI}(t) - \langle \text{RSEI} \rangle_\tau) \quad (1 \le t \le \tau). \tag{10}$$

$$\text{Range: } R(\tau) = \max_{1\le t\le\tau} X(t,\tau) - \min_{1\le t\le\tau} X(t,\tau) \quad (\tau = 1,\ 2,\ \ldots,\ n). \tag{11}$$

$$\text{Standard deviation: } S(\tau) = \left[\frac{1}{\tau}\sum_{t=1}^{\tau} (\text{RSEI}(t) - \langle \text{RSEI} \rangle_\tau)^2\right]^{1/2} \quad (\tau = 1,\ 2,\ \ldots,\ n). \tag{12}$$

If there exists $R(\tau)/S(\tau) \propto \tau^H$, then the Hurst phenomenon exists in time series (RSEI(t)), where H is the Hurst exponent. The Hurst exponent value can be fitted by the least square method in double logarithmic coordinate system (ln(τ), ln($R(\tau)/S(\tau)$)), and its value ranges from 0.00 to 1.00.

When 0.00<H<0.50 (where H is the value of Hurst exponent), the long-term correlation of eco-environmental quality in time series is characterized by anti-sustainability; the smaller the value, the stronger the anti-sustainability. When H=0.50, there is no long-term correlation of eco-environmental quality in time series. When 0.50<H<1.00, the long-term correlation in time series is characterized by persistence; the larger the value, the stronger the persistence. The Hurst exponent and the Theil-Sen median trend were superimposed to analyze the future trend of eco-environmental quality. We classified the future trend of eco-environmental quality following the classification standard of Zhang et al. (2021b), as shown in Table 3.

Table 3 Classification standard for the future trend analysis of eco-environmental quality based on the Hurst exponent and the Theil-Sen median trend

Classification standard	Future trend of eco-environmental quality
β>0.0005 and 0.65<H≤1.00	Strong persistent improvement
β>0.0005 and 0.50<H≤0.65	Weak persistent improvement
β< –0.0005 and 0.00≤H<0.35	Strong anti-sustained degradation
β< –0.0005 and 0.35≤H<0.50	Weak anti-sustained degradation
–0.0005≤β≤0.0005	Essentially constant
β< –0.0005 and 0.65<H≤1.00	Strong persistent degradation
β< –0.0005 and 0.50<H≤0.65	Weak persistent degradation
β>0.0005 and 0.00≤H<0.35	Strong anti-sustained improvement
β>0.0005 and 0.35≤H<0.50	Weak anti-sustained improvement

Note: H is the value of Hurst exponent.

2.3.3 Geographical detector

The geographical detector, which can measure the spatial differentiation and reveal the driving force behind the differentiation mechanism, has been widely used to analyze the influencing mechanisms of various factors (Wang and Hu, 2012; Su et al., 2020). In this study, the RSEI was selected as the dependent variable, and cumulative precipitation, average temperature, average relative humidity, potential evapotranspiration, elevation, slope, aspect, nighttime-light, population density and land use type were selected as the independent variables. First, a 5.0 km×5.0 km fishing network was used to uniformly generate 207,034 points in the Three-North region, through which the dependent variable was matched with the independent variables. Then, each independent variable in 2000, 2005, 2010, 2015 and 2020 was converted into a type quantity, and each hierarchical interval was determined by the optimal q statistic (where q is the explanatory power). Among them, as a type quantity, the six types in the first level classification were used for analysis in this study. Finally, the effects of each factor on the spatial distribution of the RSEI in 2000, 2005, 2010, 2015 and 2020 were investigated by factor detector, interaction detector and ecological detector of the geographical detector.

The factor detector evaluated the effect of different environmental factors on the spatial differentiation of eco-environmental quality by calculating the q value. The range of the q value is from 0.000 to 1.000; the higher the q value, the greater the influence.

$$q = 1 - \frac{\sum_{h=1}^{L} N_h \sigma_h^{\,2}}{N\sigma^2}, \tag{13}$$

where q represents the explanatory power; L is the number of layers of the factor; h is the classification or partition of factor Y or factor X; N_h and N are the unit numbers of class h and the entire region, respectively; and σ_h^2 and σ^2 are the variances of Y for class h and the entire region, respectively.

The interaction detector identified interaction between two factors to evaluate whether these two factors affect eco-environmental quality jointly or independently (Table 4).

Table 4 Classification standard of the interaction type of factors

Classification standard	Interaction type
$q(X1\cap X2)$<Min[$q(X1)$, $q(X2)$]	Nonlinear-weaken
Min[$q(X1)$, $q(X2)$]<$q(X1\cap X2)$<Max[$q(X1)$, $q(X2)$]	Uni-weaken
$q(X1\cap X2)$>Max[$q(X1)$, $q(X2)$]	Bi-enhance
$q(X1\cap X2)$=$q(X1)$+$q(X2)$	Independent
$q(X1\cap X2)$>$q(X1)$+$q(X2)$	Nonlinear-enhance

Note: $q(X1)$ and $q(X2)$ represent the explanatory power (q value) of factors $X1$ and X2 for eco-environmental quality, respectively; $q(X1\cap X2)$ represents the explanatory power (q value) for eco-environmental quality when factors $X1$ and $X2$ interact.

The ecological detector was used to determine whether the two factors had significant differences in the spatial distribution of eco-environmental quality. This was tested using the F statistic as follows:

$$F = \frac{N_{X1}(N_{X2}-1)\sum_{h=1}^{L1} N_h {\sigma_h}^2}{N_{X2}(N_{X1}-1)\sum_{h=1}^{L2} N_h {\sigma_h}^2}, \tag{14}$$

where N_{X1} and N_{X2} represent the sample size of the two factors, respectively; and $L1$ and $L2$ represent the number of the layers of the two factors, respectively.

3 Results

3.1 Spatial distribution of eco-environmental quality

Figure 2 shows the spatial distribution of eco-environmental quality in the study area for some typical years from 2000 to 2020. The RSEI values in Northwest China were generally between 0.2 and 0.4; it had been at a low level for a long time. The eco-environmental quality in the northern slope valley of the Tianshan Mountains and the Qaidam Basin was relatively good, and the RSEI values were mostly between 0.4 and 0.8. Most of these areas had a certain degree of soil

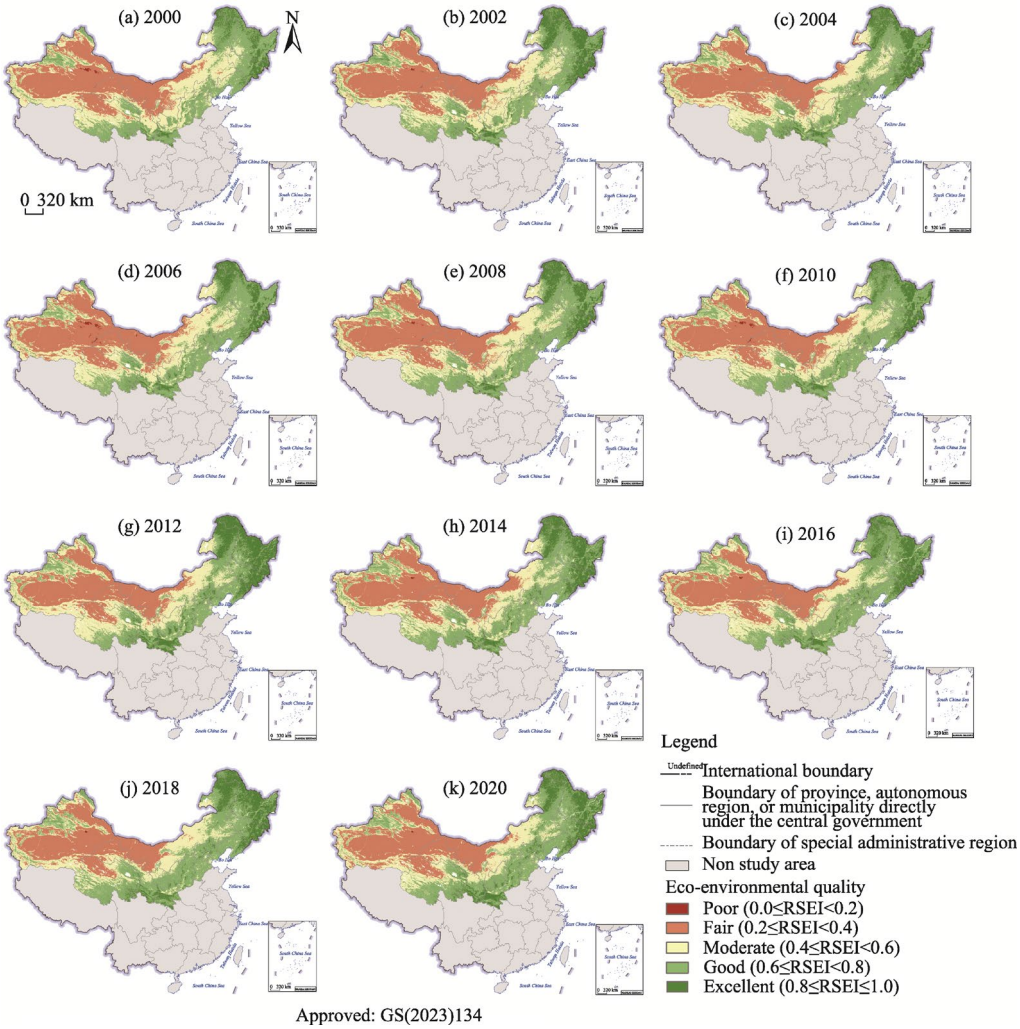

Fig. 2 Spatial distribution of eco-environmental quality (as indicated by the RSEI) in the Three-North region in 2000 (a), 2002 (b), 2004 (c), 2006 (d), 2008 (e), 2010 (f), 2012 (g), 2014 (h), 2016 (i), 2018 (j) and 2020 (k)

moisture, and the surface temperature was lower than that in the desert area. The RSEI values in North China gradually increased from north to south. The RSEI values in the Alxa Plateau, the northern Hetao Plain and the Mu Us Sandy Land were mainly between 0.2 and 0.4, and those in the Hulun Buir Plateau and Otindag Sandy Land were mainly in the range of 0.4–0.6. The eco-environmental quality of the Haihe River Basin and its surrounding areas in the southern part of North China was mainly classified as good (the RSEI values ranging from 0.6 to 0.8). The eco-environmental quality of Northeast China was mostly classified as good (the RSEI values of 0.6–0.8) or excellent (the RSEI values of 0.8–1.0). The RSEI values of the Yilehuli Mountain, Lesser Khingan Mountains and Changbai Mountains were relatively high, generally higher than 0.8.

The RSEI values in the Three-North region from 2000 to 2020 were classified and counted (Fig. 3). There were obvious differences in the percentage of the area with various RSEI values in different regions. Approximately 39.00%–45.50% of the area in Northwest China had RSEI values between 0.2 and 0.4, while approximately 21.80%–33.20% of the area had RSEI values greater than 0.6. Compared with Northwest China, the percentage of the area in North China with RSEI values below 0.4 was smaller while that with the RSEI values between 0.6 and 0.8 was greater. The RSEI values in Northeast China were all greater than 0.2. In Northeast China, the area with the RSEI values ranging from 0.2 to 0.4 accounted for approximately 0.20%–0.50% of the total area in this region, in which eco-environmental quality was considered as fair, while eco-environmental quality in the remainder region was classified as moderate, good or excellent. From 2000 to 2020, the percentage of the area classified at each RSEI level in the study area changed to different degrees, but the RSEI exhibited a fluctuating upward trend overall and its annual mean growth rate was 0.0016/a. The mean RSEI values were between 0.5 and 0.6 from 2000 to 2020 in the Three-North region, with the minimum value occurring in 2000 and the maximum in 2012.

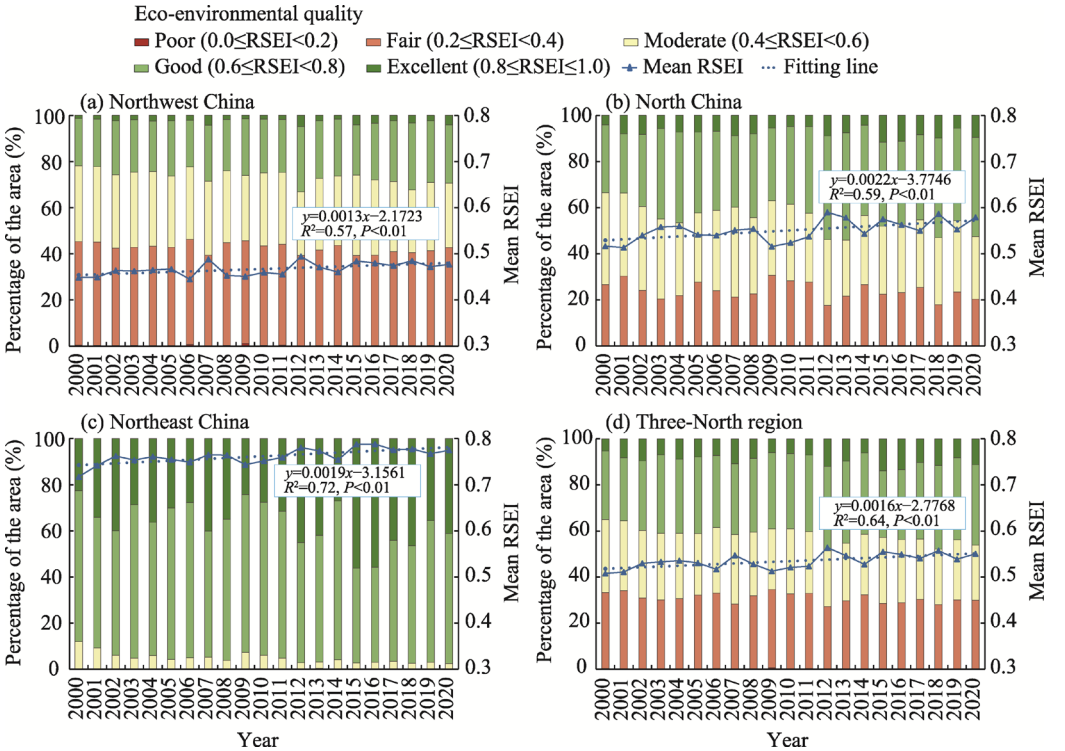

Fig. 3 Percentage of the area with different eco-environmental quality degrees (as indicated by the RSEI values) and the mean RSEI in Northwest China (a), North China (b), Northeast China (c) and the Three-North region (d) from 2000 to 2020

3.2 Dynamic tendency of eco-environmental quality

The statistical results of the variation trend of eco-environmental quality from 2000 to 2020 are shown in Table 5. During the study period, approximately 56.92% of the area in Northwest China showed an improving trend in eco-environmental quality. According to the RSEI, Northwest China also contained the largest area with slight improvement in eco-environmental quality, at 1,051,168 km^2 (accounting for 34.94% of Northwest China), followed by the area with basically stable eco-environmental quality, accounting for 34.13% of Northwest China. More than 75.00% of the areas in North China and Northeast China respectively showed an improving trend in eco-environmental quality. The areas with slightly and significantly improved eco-environmental quality in North China were 677,542 km^2 and 491,153 km^2, accounting for 44.70% and 32.41% of the total area in this region, respectively. In Northeast China, the areas with slight and significant improvement in eco-environmental quality were 256,214 km^2 and 335,402 km^2, respectively, at percentages of 32.55% and 42.61%, respectively. The significantly degraded areas in Northwest China, North China and Northeast China were 41,949, 21,793 and 11,238 km^2, respectively, accounting for 1.41% of the total study area (the Three-North region). In terms of the overall values, 7.79% of the total area exhibited a degradation trend in eco-environmental quality in the Three-North region, and the main trend of eco-environmental quality from 2000 to 2020 was basically stable or improved (accounting for 26.82% and 65.39%, respectively).

Table 5 Statistical results of the variation trend in eco-environmental quality from 2000 to 2020

Variation trend	Northwest China		North China		Northeast China		Three-North region	
	Area (km^2)	Percentage (%)	Area (km^2)	Percentage (%)	Area (km^2)	Percentage (%)	Area (km^2)	Percentage (%)
Significant degradation	41,949	1.39	21,793	1.44	11,238	1.43	75,190	1.41
Slight degradation	227,387	7.56	78,656	5.19	32,731	4.16	339,363	6.38
Basically stable	1,026,679	34.13	246,460	16.26	151,471	19.25	1,426,634	26.82
Slight improvement	1,051,168	34.94	677,542	44.70	256,214	32.55	1,987,808	37.38
Significant improvement	661,078	21.98	491,153	32.41	335,402	42.61	1,489,976	28.01

According to the spatial distribution of the variation trend of eco-environmental quality (Fig. 4), the areas exhibiting a basically stable trend of eco-environmental quality in Northwest China were distributed in the Tarim Basin, Junggar Basin, Kumtag Desert and Qaidam Basin. Similarly, eco-environmental quality in the Badain Jaran Desert, Alxa Plateau and the surrounding areas of Central Gobi also remained basically stable. These areas are mainly desert and Gobi regions with low soil moisture content, high surface temperature, and poor eco-environmental quality for a long time. With high vegetation coverage and relatively stable ecosystems, eco-environmental quality of the Lesser Khingan Mountains and Changbai Mountains in Northeast China remained basically stable at a good level. The areas north of the Yarkant River Basin and Tarim River Basin, the Loess Plateau and the Northeast China Plain (Songnen Plain, Liaohe River Plain and Sanjiang Plain) mainly showed a significant improvement in eco-environmental quality. However, there were some areas showing significant degradation trend of eco-environmental quality in Northwest China, North China and Northeast China. In Northwest China, these areas were mainly distributed in the Halktawu Mountain and Boluokenu Mountain (Fig. 4a); in North China, they were mainly distributed in areas with rapid economic development, such as Beijing-Tianjin-Hebei region (Fig. 4b). In addition, the northernmost end of the border between Inner Mongolia Autonomous Region and Heilongjiang Province (Fig. 4c), that is, the eastern side of the Ergun River and the western side of the Mohe City, also showed significant degradation in eco-environmental quality.

The Hurst exponent was superimposed and analyzed with the results of Theil-Sen median trend analysis to obtain the persistence of the future trend in eco-environmental quality in the Three-North region (Fig. 5). The Hurst exponent of the RSEI in the Three-North region ranged

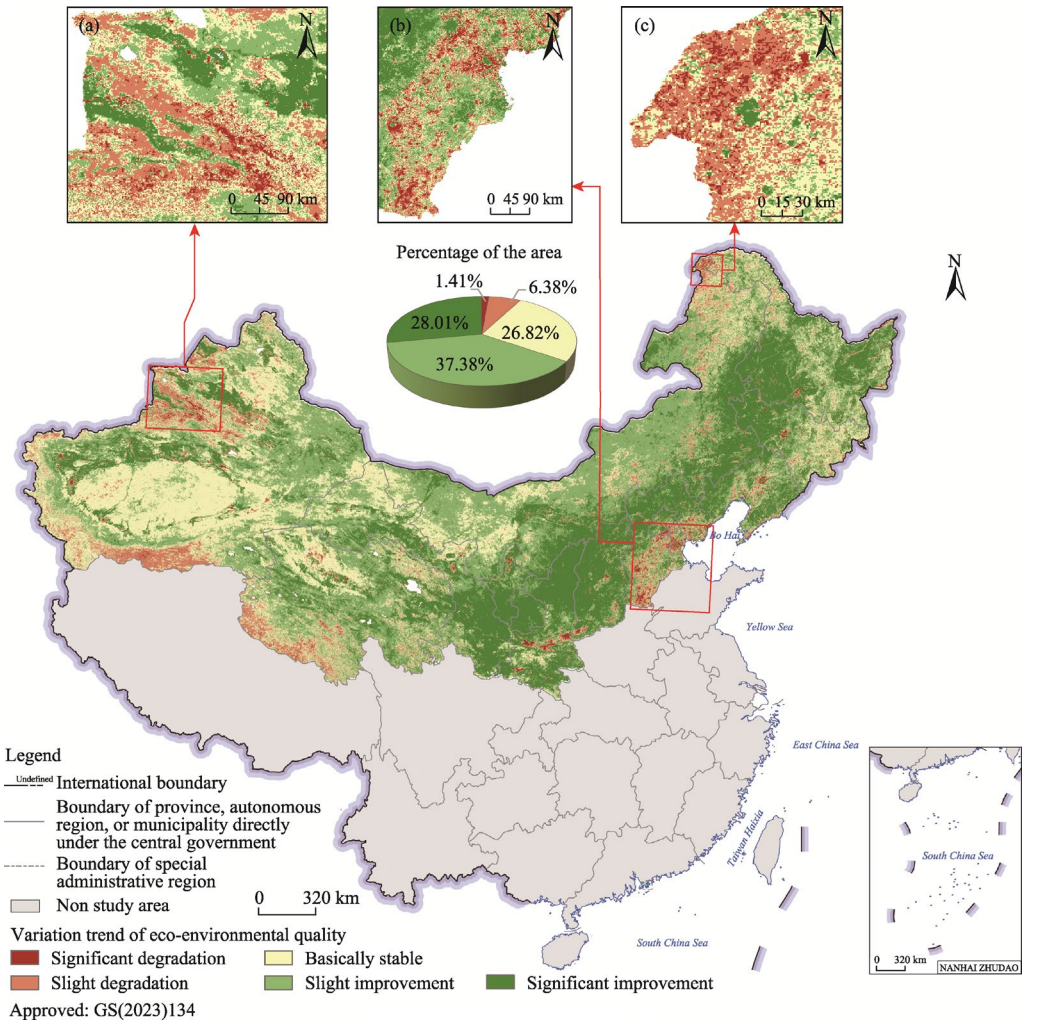

Fig. 4 Spatial distribution of the variation trend of eco-environmental quality in the Three-North region from 2000 to 2020. The pie chart shows the percentage of the area occupied by different variation trends of eco-environmental quality. (a), (b) and (c) show the partial enlargement of the spatial distribution of the variation trend of eco-environmental quality.

from 0.20 to 0.76, with an average of 0.53, and the percentages of the area with persistence and anti-sustainability in eco-environmental quality were 63.55% and 36.44%, respectively (Fig. 5a). The overall future trend of eco-environmental quality in the Three-North region was weak, mainly dominated by weak persistence, followed by weak anti-sustainability, accounting for 52.47% and 35.24% of the total study area, respectively, indicating that the future trend of eco-environmental quality in most areas may be reversed. The percentage of the area with strong persistence in eco-environmental quality was 11.08%, mainly located in the eastern Loess Plateau, the Songnen Plain and the Liaohe River Plain. As shown in Figure 5b, 0.81% of the Three-North region showed strong persistent degradation in eco-environmental quality, 0.31% exhibited strong anti-sustained improvement, 10.09% showed strong persistent improvement and 0.13% showed strong anti-sustained degradation. The overall future changes of eco-environmental quality in the Three-North region were mainly based on improvement in the RSEI, but they were not strong in sustainability. The percentages of the area with weak anti-sustained improvement and weak persistent degradation in eco-environmental quality (the RSEI might decrease) in the Three-North region were 16.23% and 3.78%, respectively. The areas with weak persistent improvement and weak anti-sustained degradation in eco-environmental

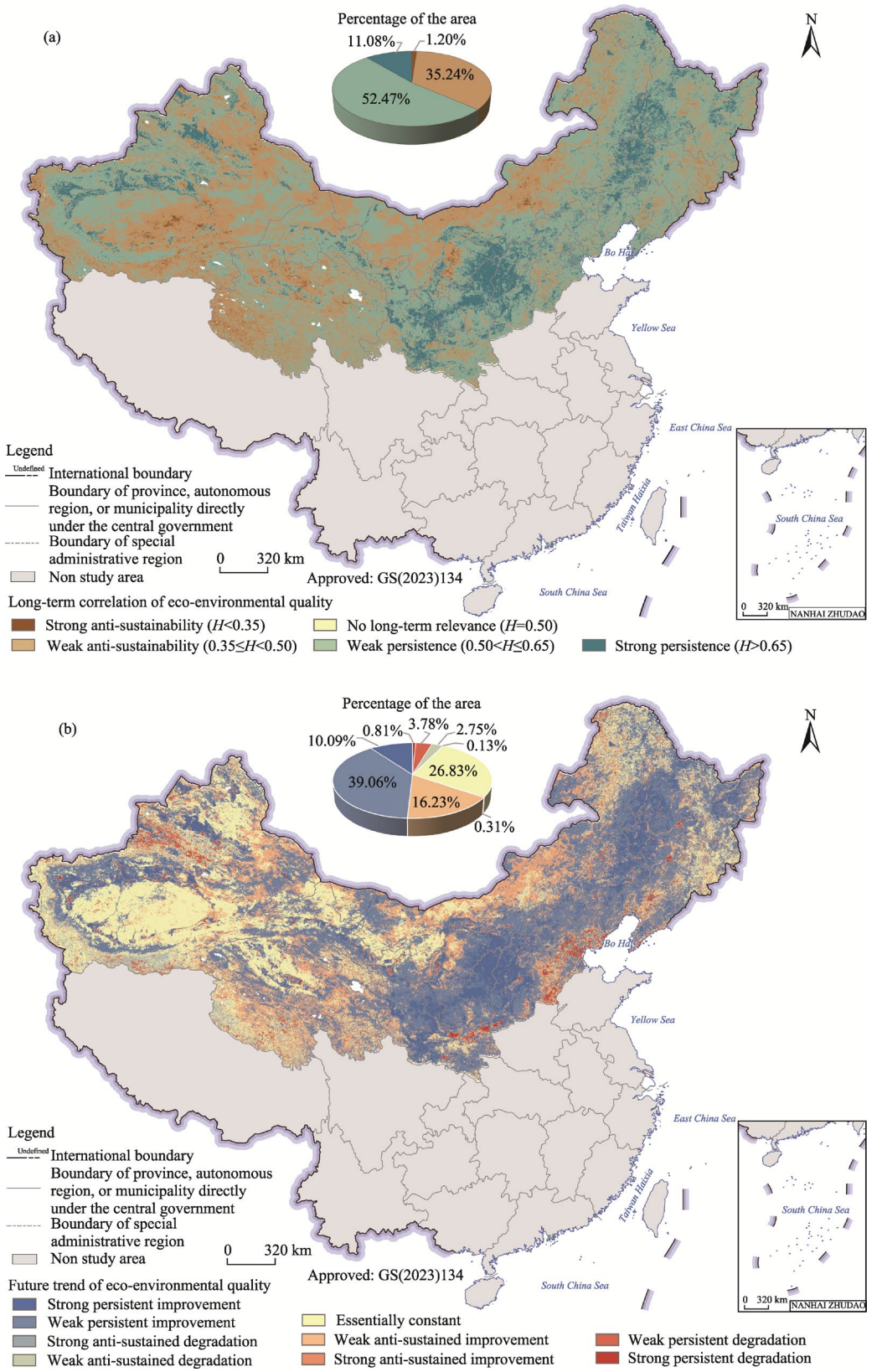

Fig. 5 Spatial distribution of the long-term correlation of eco-environmental quality in time series (indicated by the Hurst exponent (*H*); a) and the future trend of eco-environmental quality (b) in the Three-North region

quality (the RSEI might increase) accounted for 39.06% and 2.75% of the Three-North region, respectively. In the future, the areas where the RSEI would remain essentially constant are mainly distributed in the Tarim Basin, the Junggar Basin, the Qaidam Basin, the Badain Jaran Desert, the Alxa Plateau and the surroundings of the Central Gobi; these expectations are highly consistent with the variation trend over the past 21 years (2000–2020). The eco-environmental quality of the Halktawu Mountain, Boluokenu Mountain and Beijing-Tianjin-Hebei region may also continue to degrade to varying degrees in the future.

3.3 Analysis between influencing factors and eco-environment quality

Ten influencing factors, including cumulative precipitation, average temperature, average relative humidity, potential evapotranspiration, elevation, slope, aspect, nighttime-light, population density and land use type, were selected and their impacts on the spatial distribution of eco-environmental quality in the Three-North region were explored by the geographical detector. The explanatory power q values of the influencing factors were obtained, as shown in Figure 6. Based on these results, the driving effect of each influencing factor on the spatial distribution pattern of eco-environmental quality was different. From 2000 to 2020, the q value of average relative humidity was the largest among the ten influencing factors, followed by cumulative precipitation, land use type and potential evapotranspiration. The q value of average relative humidity was greater than 0.870, indicating that average relative humidity had a great impact on the formation and change in the spatial distribution of eco-environmental quality. In addition, cumulative precipitation and land use type were the subdominant factors affecting the spatial distribution of eco-environmental quality in the Three-North region, with q values of approximately 0.730 and 0.560, respectively. The q values of potential evapotranspiration fluctuated around 0.410 and decreased to a greater extent in 2015. The other influencing factors had relatively small effects on the spatial distribution of eco-environmental quality, with q values less than 0.300. Among them, aspect had the weakest effect on the spatial distribution pattern of eco-environmental quality, with q value of only approximately 0.010. In general, the explanatory power of meteorological factors on the spatial distribution of eco-environmental quality was stronger than that of topographic and socioeconomic factors. The effects of anthropogenic factors, such as population density and land use type, on eco-environmental quality gradually increased over time.

A two-factor interaction would enhance the explanatory power of influencing factors on the spatial distribution of eco-environmental quality (Fig. 7). From 2000 to 2020, the interaction types between the influencing factors were mainly double synergy (bi-enhance) and nonlinear synergy (nonlinear enhance), and there were no factors to act independently. We arranged the

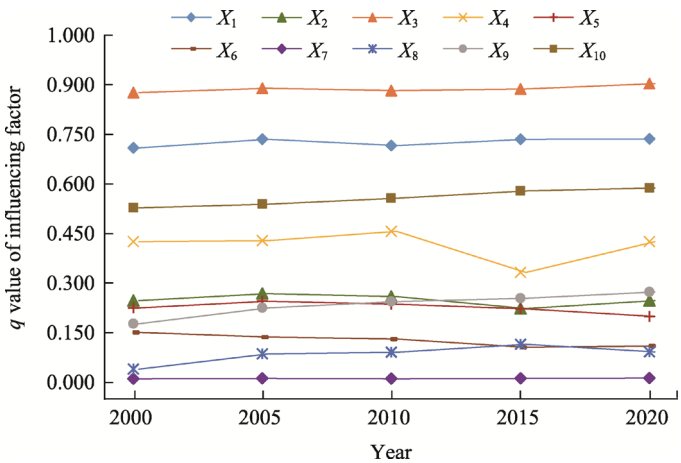

Fig. 6 Explanatory power q values of cumulative precipitation (X_1), average temperature (X_2), average relative humidity (X_3), potential evapotranspiration (X_4), elevation (X_5), slope (X_6), aspect (X_7), nighttime-light (X_8), population density (X_9), and land use type (X_{10}) in 2000, 2005, 2010, 2015 and 2020

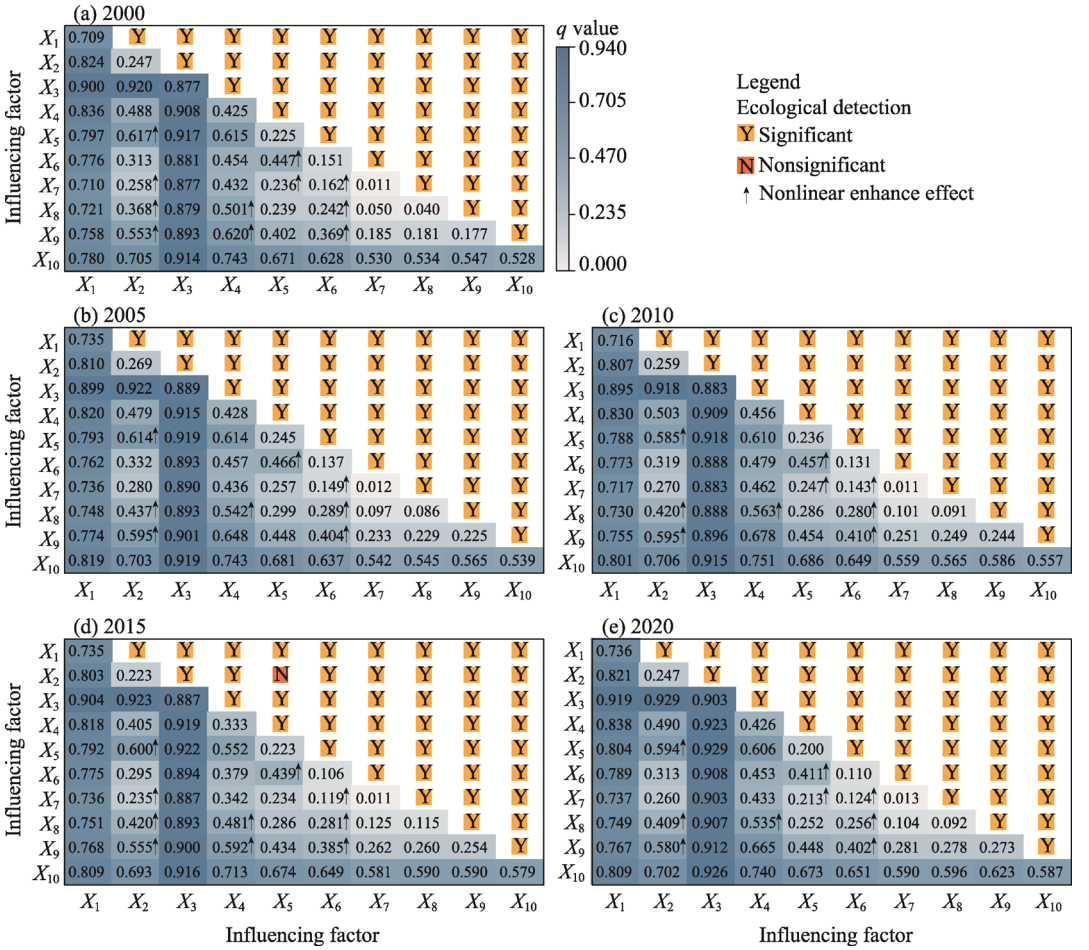

Fig. 7 Interaction detection and ecological detection results of cumulative precipitation (X_1), average temperature (X_2), average relative humidity (X_3), potential evapotranspiration (X_4), elevation (X_5), slope (X_6), aspect (X_7), nighttime-light (X_8), population density (X_9) and land use type (X_{10}) in 2000 (a), 2005 (b), 2010 (c), 2015 (d) and 2020 (e). The ↑ means that the interaction between two influencing factors is nonlinear enhance effect and no ↑ means that the interaction between two influencing factors is bi-enhance effect.

explanatory force of the factor interaction in five representative years according to the q values. The most dominant interaction factors were the combination of average temperature and average relative humidity in 2000, 2005, 2010, 2015 and 2020, with q values of 0.920, 0.922, 0.918, 0.923 and 0.929, respectively. In addition, the q values of average relative humidity∩potential evapotranspiration, average relative humidity∩elevation, and average relative humidity∩land use type were all greater than 0.900. Average relative humidity was the dominant meteorological factor on the spatial distribution of eco-environmental quality and made the greatest contribution to the change in the distribution pattern, including interactions with other influencing factors. The q values of elevation and population density were low, but the explanatory power between them was stronger than that of the other single factors when interacting with meteorological factors. The interaction between slope and other influencing factors was mostly nonlinearly enhanced. In addition, the explanatory power of topographic and socioeconomic factors was weak when acting as single factors, and the power remained low after a two-factor interaction. Topographic and socioeconomic factors presented bi-enhance effect and nonlinear enhance effect when interacting with meteorological factors, indicating that the influence of topographic and socioeconomic factors on the spatial distribution of eco-environmental quality was neither unilateral nor simply superposed with meteorological factors. In addition, the ecological detection of each factor was

performed to detect whether there were significant differences in the impact of the two factors on the spatial distribution of eco-environmental quality (Fig. 7). According to the detection results, except for average temperature and elevation that were not significantly different in 2015, all the other factors differed significantly and had different influence mechanisms on the spatial distribution of eco-environmental quality.

4 Discussion

4.1 Variation trend of eco-environmental quality

According to the variation trend analysis results (Fig. 4), areas with significant degradation in eco-environmental quality were found in Northwest China, North China and Northeast China from 2000 to 2020. In Northwest China, these areas were mainly concentrated on both sides of the geometric center of the Tianshan Mountains. Zhou et al. (2020) showed that high altitude, low precipitation, dry climate and fragile vegetation are the main causes for the degradation of eco-environmental quality in this area. Meanwhile, there were obvious regional differences in eco-environmental quality in the Beijing-Tianjin-Hebei region of North China, generally exhibiting an improvement pattern to the northwest while a degradation pattern to the southeast. Due to the strengthening of artificial ecological protection policies, eco-environmental quality in Zhangjiakou City, Chengde City and other places has been improved (Deng et al., 2018; Ji et al., 2020). Although ecological restoration projects are conducive to the benign development of eco-environmental quality (Xu et al., 2020), areas with dense populations, convenient transportation and strong human disturbance are not suitable for vegetation restoration (Zhang et al., 2017), resulting in a decline in eco-environmental quality in the southeastern Hebei Province (such as Handan and Hengshui cities) and Tianjin. Located in the northern end of China, a small area on the east side of the Ergun River experienced a decline in eco-environmental quality due to extreme climatic conditions. Since the implementation of the Three-North Shelterbelt Program, the overall eco-environmental quality of the Three-North region was improved. However, a significant degradation trend in eco-environmental quality in some regions existed, and eco-environmental quality might continue to degrade in the future (Fig. 5b). The change in eco-environmental quality was affected by many factors, such as climate change, land use and population density (Yuan et al., 2021), but the reasons for the degradation in eco-environmental quality varied from region to region. In the future, ecological protection policies should be formulated according to the main factors affecting the degradation of eco-environmental quality in each area. For areas with harsh climatic conditions and fragile vegetation ecology, such as the edge of the oases in the northern and southern Tianshan Mountains, attention should be paid to ecological water use and strict protection of the natural surroundings (Zheng and Zhu, 2017). For areas with rapid economic development, such as the Beijing-Tianjin-Hebei region, some measures should be considered to restore key vegetation in regions with intensive human disturbance (Yuan et al., 2021). For areas with better natural conditions and abundant resources, such as the Greater Khingan Mountains and Changbai Mountains, priority should be given to protection and categorical management to promote ecological restoration and functional reconstruction (Wang et al., 2020).

4.2 Factors influencing the spatial distribution of eco-environmental quality

The interaction between natural factors is complex, and it is difficult to ensure that each factor is independent of each other. Therefore, analytical methods will be considered relatively more in the driver analysis to reveal the independent effects of factors as much as possible. In contrast to correlation and partial correlation analyses, the geographical detector has no assumption of linearity and is essentially free of multicollinearity, with each factor having an independent effect on the result. The geographical detector can diagnose the independent driving force of geographical variables, but its application in eco-environmental quality analysis is still relatively rare. In this study, ten influencing variables from two categories of natural and anthropogenic

factors were analyzed to determine the drivers of the spatial differentiation of eco-environmental quality by the geographical detector. To make the result of the geographical detector as accurate as possible, we uniformly generated a total of 207,034 points in the Three-North region to match the RSEI with each influencing factor. The hierarchical interval of continuous variables has direct or indirect effects on the q value (Wang et al., 2010; Su et al., 2020). Therefore, in the discretization of the continuous variables, the q statistic was used to prefer parameters, such as discrete methods and the number of levels, and determine the hierarchical interval of each influencing factor. The larger the q value, the better the partition effect (Su et al., 2020).

Based on the factor detection results (Fig. 6), average relative humidity and accumulated precipitation had strong explanatory power for the spatial distribution of eco-environmental quality, while average temperature had weak explanatory power. Most of the Three-North region is located in arid and semi-arid climate zones. Temperature mainly regulated the annual growth law of vegetation. Compared with precipitation, the correlation between temperature and interannual variation in vegetation was generally low, and vegetation was more sensitive to the influence of precipitation and humidity (Xie et al., 2016). In addition, the influence of anthropogenic factors such as population density and land use type on the spatial distribution of eco-environmental quality gradually increased over time, which is consistent with the findings of Chun et al. (2018) and Ji et al. (2020), supporting the reasonableness of the factor detection results. The results of interaction detection (Fig. 7) showed that the interaction between each two drivers (factors) had a greater impact on the spatial distribution of eco-environmental quality than a single driver (factor). Topographic factors (e.g., elevation and slope) had a moderate effect on the spatial distribution of eco-environmental quality under the action of a single factor, but their degree of influence was enhanced when interacting with meteorological factors. This suggested that multiple drivers (factors) comprehensively affect the quality of the regional eco-environment (Dai et al., 2020). However, when exploring the explanatory power of each influencing factor on the spatial distribution of eco-environmental quality, we only discussed the global factor responses of five key years (2000, 2005, 2010, 2015 and 2020) in the entire Three-North region without further dividing the study area or analyzing the local driving forces of different regions on an annual scale. In follow-up studies, the spatial and temporal resolution of the analysis should be improved, and the specific response of each influencing factor in different regions should be discussed in depth.

4.3 Limitations and prospects

GEE is capable of rapidly batch-processing large numbers of MODIS or Landsat images, which is an improvement on the tedious calculation process of the RSEI in large-scale applications (Huang et al., 2021; Xiong et al., 2021). In this study, the RSEI was used to evaluate eco-environmental quality in the Three-North region. The four indicators (NDVI, Wet, NDBSI and LST) used to construct the RSEI had certain loadings on the first principal component. Unlike the positive and negative uncertainties of the loadings of the four indicators on the second, third and fourth principal components, the eigenvectors of the greenness and humidity indicators on the first principal component were always positive, while the eigenvectors of dryness and heat were always negative (data not shown). In addition, the eigenvalue of the first principal component had a contribution rate of more than 70.00% in all years, and it integrated most of the characteristics of the four indicators, which could reflect the eco-environment condition more reasonably. The spatial distribution results (Fig. 3) showed that the RSEI values in the Three-North region were generally moderate, and the percentage of the area with particularly good or poor eco-environmental quality was relatively small. The RSEI values were greater in Northeast China and lower in Northwest China, which is consistent with the results obtained by Liao et al. (2020) and Ji et al. (2022). The RSEI can effectively distinguish the ecological status of different landscapes (Wang et al., 2010), showing its effectiveness for evaluating the changes in eco-environmental quality. However, it still has some limitations. Due to the large scope of the study area, it was difficult to unify the dates of the selected MODIS images when constructing the

RSEI. Although the median synthesis method was designed to ensure the intermediate level of temporal remote sensing images as much as possible, it might have some impact on the comparability of the RSEI evaluation (Zheng et al., 2020). There has yet to be a complete solution for the instability of the RSEI time series, which greatly limits its utility in large-scale applications (Zheng et al., 2022). In addition, the evaluation method of eco-environmental quality based on the RSEI mainly focused on the four indicators of greenness, wetness, dryness and heat. However, the ecosystems are complex and diverse, involving many aspects related not only to the natural environment but also to the socioeconomic development and government management (Xiong et al., 2021; Yuan et al., 2021). How to effectively screen other key indicators and combine them with remote sensing technology is a direction for future research.

5 Conclusions

In this study, the Three-North region was selected as the research area, and MODIS images obtained from the GEE platform were used to calculate the RSEI. The Theil-Sen median trend method combined with the MK test was used to analyze the variation trend of eco-environmental quality in the Three-North region from 2000 to 2020, and the Hurst exponent and the Theil-Sen median trend were superimposed to predict the future trend of eco-environmental quality. In addition, the geographical detector was applied to quantitatively analyze the influence of different factors on the spatial distribution of eco-environmental quality.

The spatial distribution of the eco-environmental quality in the Three-North region exhibited obvious regional characteristics. Eco-environmental quality had been at a low level for a long time in Northwest China, gradually increased from north to south in North China, and was relatively good in Northeast China. From 2000 to 2020, the average RSEI values in the Three-North region increased at an average growth rate of 0.0016/a. Eco-environmental quality in the Three-North region showed the spatial distribution characteristics of overall improvement and local degradation. The persistence of future change in eco-environmental quality was stronger than the anti-sustainability. Eco-environmental quality may be mainly improved in the future, but the overall trend is weak, and there is a possibility of reversal in some local regions. Thus, it is necessary to continue to strengthen the protection of the ecological environment in the Three-North region. Average relative humidity, accumulated precipitation and land use type were the dominant factors determining the spatial distribution of eco-environmental quality in the Three-North region. The explanatory power of meteorological factors on the spatial distribution of eco-environmental quality was stronger than that of topographic factors. With passage of time, the influence of anthropogenic factors such as population density and land use type on eco-environmental quality gradually increased. The two-factor interaction was dominated by the bi-enhance effect, and the interaction strengthened the explanatory power of the spatial distribution of eco-environmental quality, among which the interaction of average temperature∩average relative humidity was the highest.

In the Three-North region, the ecological restoration project is conducive to the benign development of eco-environmental quality; however, there are still some areas with degraded eco-environmental quality. Generally, eco-environmental quality is influenced by a combination of driving factors, and in the future, ecological protection policies should be formulated according to the main factors affecting the degradation of eco-environmental quality in various areas. This study reasonably reflects the eco-environmental quality of the Three-North region by constructing the RSEI, but the stability of the RSEI time series needs further improvement for large-scale applications.

Acknowledgements

This research was supported by the National Natural Science Foundation of China (31971578), the Scientific Research Fund of Changsha Science and Technology Bureau (kq2004095), the National Bureau to Combat

Desertification, State Forestry Administration of China (101-9899), the Training Fund of Young Professors from Hunan Provincial Education Department (90102-7070220090001) and the Postgraduate Scientific Research Innovation Project of Hunan Province (CX20220707). We also thank the editors and anonymous reviewers for their constructive comments.

References

Adrian J, Sagan V, Maimaitijiang M. 2021. Sentinel SAR-optical fusion for crop type mapping using deep learning and Google Earth Engine. ISPRS Journal of Photogrammetry and Remote Sensing, 175: 215–235.

Al-Quraishi A M F, Gaznayee H A, Crespi M. 2021. Drought trend analysis in a semi-arid area of Iraq based on Normalized Difference Vegetation Index, Normalized Difference Water Index and Standardized Precipitation Index. Journal of Arid Land, 13(4): 413–430.

Arshad S, Ahmad S R, Abbas S, et al. 2022. Quantifying the contribution of diminishing green spaces and urban sprawl to urban heat island effect in a rapidly urbanizing metropolitan city of Pakistan. Land Use Policy, 113: 105874, doi: 10.1016/j.landusepol.2021.105874.

Cao S X, Suo X H, Xia C Q. 2020. Payoff from afforestation under the Three-North Shelter Forest Program. Journal of Cleaner Production, 256(C): 120461, doi: 10.1016/j.jclepro.2020.120461.

Chun X, Yong M, Liu J Y, et al. 2018. Monitoring land cover change and its dynamic mechanism on the Qehan Lake Basin, Inner Mongolia, North China, during 1977–2013. Environmental Monitoring and Assessment, 190(4): 205, doi: 10.1007/s10661-018-6582-x.

Dai X A, Gao Y, He X W, et al. 2020. Spatial-temporal pattern evolution and driving force analysis of ecological environment vulnerability in Panzhihua City. Environmental Science and Pollution Research International, 28(6): 7151–7166.

Deng C L, Zhang B Q, Cheng L Y, et al. 2019. Vegetation dynamics and their effects on surface water-energy balance over the Three-North Region of China. Agricultural and Forest Meteorology, 275: 79–90.

Deng Y, Jiang W G, Wang W J, et al. 2018. Urban expansion led to the degradation of habitat quality in the Beijing-Tianjin-Hebei Area. Acta Ecologica Sinica, 38(12): 4516–4525. (in Chinese)

Duan H C, Yan C Z, Tsunekawa A, et al. 2011. Assessing vegetation dynamics in the Three-North Shelter Forest region of China using AVHRR NDVI data. Environmental Earth Sciences, 64(4): 1011–1020.

Erasmi S, Klinge M, Dulamsuren C. 2021. Modelling the productivity of Siberian larch forests from Landsat NDVI time series in fragmented forest stands of the Mongolian forest-steppe. Environmental Monitoring and Assessment, 193(4): 200, doi: 10.1007/S10661-021-08996-1.

Floreano I X, de Moraes L A F. 2021. Land use/land cover (LULC) analysis (2009–2019) with Google Earth Engine and 2030 prediction using Markov-CA in the Rondônia State, Brazil. Environmental Monitoring and Assessment, 193(4): 239, doi: 10.1007/s10661-021-09016-y.

Gao P W, Kasimu A, Zhao Y Y, et al. 2020. Evaluation of the temporal and spatial changes of ecological quality in the Hami Oasis based on RSEI. Sustainability, 12(18): 7716, doi: 10.3390/su12187716.

Gorelick N, Hancher M, Dixon M, et al. 2017. Google Earth Engine: Planetary-scale geospatial analysis for everyone. Remote Sensing of Environment, 202: 18–27.

Hong J H, Su Z L T, Lu E H C. 2020. Spatial perspectives toward the recommendation of remote sensing images using the INDEX indicator, based on principal component analysis. Remote Sensing, 12(8): 1277, doi: 10.3390/rs12081277.

Hu L, Fan W J, Yuan W P, et al. 2021. Spatiotemporal variation of vegetation productivity and its feedback to climate change in Northeast China over the last 30 years. Remote Sensing, 13(5): 951, doi: 10.3390/rs13050951.

Hu X S, Xu H Q. 2018. A new remote sensing index for assessing the spatial heterogeneity in urban ecological quality: A case from Fuzhou City, China. Ecological Indicators, 89: 11–21.

Huang H P, Chen W, Zhang Y, et al. 2021. Analysis of ecological quality in Lhasa metropolitan area during 1990–2017 based on remote sensing and Google Earth Engine platform. Journal of Geographical Sciences, 31(2): 265–280.

Ji J W, Wang S X, Zhou Y, et al. 2020. Spatiotemporal change and landscape pattern variation of eco-environmental quality in Jing-Jin-Ji urban agglomeration from 2001 to 2015. IEEE Access, 8: 125534–125548.

Ji J W, Tang Z Z, Zhang W W, et al. 2022. Spatiotemporal and multiscale analysis of the coupling coordination degree between economic development equality and eco-environmental quality in China from 2001 to 2020. Remote Sensing, 14(3): 737, doi: 10.3390/rs14030737.

Jiang F G, Deng M L, Long Y, et al. 2022. Spatial pattern and dynamic change of vegetation greenness from 2001 to 2020 in Tibet, China. Frontiers in Plant Science, 13: 892625, doi: 10.3389/fpls.2022.892625.

Jiang L G, Liu Y, Wu S, et al. 2021. Analyzing ecological environment change and associated driving factors in China based on NDVI time series data. Ecological Indicators, 129: 107933, doi: 10.1016/j.ecolind.2021.107933.

Jiang W G, Yuan L H, Wang W J, et al. 2015. Spatio-temporal analysis of vegetation variation in the Yellow River Basin. Ecological Indicators, 51: 117–126.

Kutner M H, Nachtsheim C J, Neter J, et al. 2004. Applied Linear Statistical Models (5th ed.). Chicago: McGraw-Hill/Irwin, 1316.

Lee P S H, Park J. 2020. An effect of urban forest on urban thermal environment in Seoul, South Korea, based on Landsat imagery analysis. Forests, 11(6): 630, doi: 10.3390/f11060630.

Li C, Li X M, Luo D L, et al. 2021a. Spatiotemporal pattern of vegetation ecology quality and its response to climate change between 2000–2017 in China. Sustainability, 13(3): 1419, doi: 10.3390/su13031419.

Li J, Wang J L, Zhang J, et al. 2021b. Dynamic changes of vegetation coverage in China-Myanmar economic corridor over the past 20 years. International Journal of Applied Earth Observations and Geoinformation, 102: 102378, doi: 10.1016/j.jag.2021.102378.

Li S D, Feng D Q. 2021. World famous ecological project—Three North Shelterbelt System Construction Project in China. Zhejiang Forestry, (9): 9–11. (in Chinese)

Liao W H, Jiang W G, 2020. Evaluation of the spatiotemporal variations in the eco-environmental quality in China based on the remote sensing ecological index. Remote Sensing, 12(15): 2462, doi: 10.3390/rs12152462.

Liu H, Li X J, Mao F J, et al. 2021. Spatiotemporal evolution of fractional vegetation cover and its response to climate change based on MODIS data in the subtropical region of China. Remote Sensing, 13(5): 913, doi: 10.3390/rs13050913.

Liu J Y, Zhang Z X, Xu X L, et al. 2010. Spatial patterns and driving forces of land use change in China during the early 21st century. Journal of Geographical Sciences, 20(4): 483–494.

Lu F, Hu H F, Sun W J, et al. 2018. Effects of national ecological restoration projects on carbon sequestration in China from 2001 to 2010. Proceedings of the National Academy of Sciences of the United States of America, 115(16): 4039–4044.

Mishra V K, Pant T. 2020. Open surface water index: a novel approach for surface water mapping and extraction using multispectral and multisensory data. Remote Sensing Letters, 11(11): 973–982.

Nietupski T C, Kennedy R E, Temesgen H, et al. 2021. Spatiotemporal image fusion in Google Earth Engine for annual estimates of land surface phenology in a heterogenous landscape. International Journal of Applied Earth Observations and Geoinformation, 99: 102323, doi: 10.1016/j.jag.2021.102323.

Pekel J F, Cottam A, Gorelick N, et al. 2016. High-resolution mapping of global surface water and its long-term changes. Nature, 540(7633): 418–422.

Rivas-Tabares D A, Saa-Requejo A, Martín-Sotoca J J. 2021. Multiscaling NDVI series analysis of rainfed cereal in Central Spain. Remote Sensing, 13(4): 568, doi: 10.3390/rs13040568.

Saleh S K, Amoushahi S, Gholipour M. 2021. Spatiotemporal ecological quality assessment of metropolitan cities: a case study of central Iran. Environmental Monitoring and Assessment, 193(5): 305, doi: 10.1007/s10661-021-09082-2.

Shan W, Jin X B, Ren J, et al. 2019. Ecological environment quality assessment based on remote sensing data for land consolidation. Journal of Cleaner Production, 239(C): 118126, doi: 10.1016/j.jclepro.2019.118126.

Su Y, Li T X, Cheng S K, et al. 2020. Spatial distribution exploration and driving factor identification for soil salinisation based on geodetector models in coastal area. Ecological Engineering, 156: 105961, doi: 10.1016/j.ecoleng.2020.105961.

Sun C J, Li X M, Zhang W Q, et al. 2020. Evolution of ecological security in the Tableland Region of the Chinese Loess Plateau using a remote-sensing-based index. Sustainability, 12(8): 3489, doi: 10.3390/su12083489.

Venkatappa M, Sasaki N, Han P, et al. 2021. Impacts of droughts and floods on croplands and crop production in Southeast Asia – An application of Google Earth Engine. Science of the Total Environment, 795: 148829, doi: 10.1016/J.SCITOTENV.2021.148829.

Wang C L, Jiang Q O, Deng X Z, et al. 2020. Spatio-temporal evolution, future trend and phenology regularity of net primary productivity of forests in Northeast China. Remote Sensing, 12(21): 3670, doi: 10.3390/rs12213670.

Wang H N, Zhang M Y, Cui L J, et al. 2019. Evaluation of ecological environment quality of Hengshui Lake Wetlands based on DPSIR model. Wetland Science, 17(2): 193–198. (in Chinese)

Wang J F, Li X H, Christakos G, et al. 2010. Geographical detectors-based health risk assessment and its application in the neural tube defects study of the Heshun Region, China. International Journal of Geographical Information Science, 24(1): 107–27.

Wang J F, Hu Y. 2012. Environmental health risk detection with GeogDetector. Environmental Modelling and Software, 33: 114–115.

Wen X L, Ming Y L, Gao Y G, et al. 2019. Dynamic monitoring and analysis of ecological quality of Pingtan Comprehensive

Experimental Zone, a new type of Sea Island City, based on RSEI. Sustainability, 12(1): 21, doi: 10.3390/su12010021.

Xie B N, Jia X X, Qin Z F, et al. 2016. Vegetation dynamics and climate change on the Loess Plateau, China: 1982–2011. Regional Environmental Change, 16(6): 1583–1594.

Xiong Y, Xu W H, Lu N, et al. 2021. Assessment of spatial-temporal changes of ecological environment quality based on RSEI and GEE: A case study in Erhai Lake Basin, Yunnan province, China. Ecological Indicators, 125: 107518, doi: 10.1016/J.ECOLIND.2021.107518.

Xu D, Yang F, Yu L, et al. 2021. Quantization of the coupling mechanism between eco-environmental quality and urbanization from multisource remote sensing data. Journal of Cleaner Production, 321: 128948, doi: 10.1016/J.JCLEPRO.2021.128948.

Xu H Q, Wang M Y, Shi T T, et al. 2018. Prediction of ecological effects of potential population and impervious surface increases using a remote sensing based ecological index (RSEI). Ecological Indicators, 93: 730–740.

Xu H Q, Wang Y F, Guan H D, et al. 2019. Detecting ecological changes with a remote sensing based ecological index (RSEI) produced time series and change vector analysis. Remote Sensing, 11(20): 2354, doi: 10.3390/rs11202345.

Xu K P, Chi Y Y, Wang J J, et al. 2020. Analysis of the spatial characteristics and driving forces determining ecosystem quality of the Beijing-Tianjin-Hebei region. Environmental Science and Pollution Research International, 28(10): 12555–12565.

Yuan B D, Fu L N, Zou Y A, et al. 2021. Spatiotemporal change detection of ecological quality and the associated affecting factors in Dongting Lake Basin, based on RSEI. Journal of Cleaner Production, 302: 126995, doi: 10.1016/J.JCLEPRO.2021.126995.

Zhang D, Huang Q X, He C Y, et al. 2017. Impacts of urban expansion on ecosystem services in the Beijing-Tianjin-Hebei urban agglomeration, China: A scenario analysis based on the Shared Socioeconomic Pathways. Resources, Conservation & Recycling, 125: 115–130.

Zhang D N, Zuo X X, Zang C F. 2021a. Assessment of future potential carbon sequestration and water consumption in the construction area of the Three-North Shelterbelt Programme in China. Agricultural and Forest Meteorology, 303: 108377, doi: 10.1016/J.AGRFORMET.2021.108377.

Zhang W Q, Jin H A, Shao H Y, et al. 2021b. Temporal and spatial variations in the leaf area index and its response to topography in the Three-River Source Region, China from 2000 to 2017. ISPRS International Journal of Geo-Information, 10(1): 33, doi: 10.3390/IJGI10010033.

Zheng X, Zhu J J. 2017. A new climatic classification of afforestation in Three-North regions of China with multi-source remote sensing data. Theoretical and Applied Climatology, 127(1–2): 465–480.

Zheng Z H, Wu Z F, Chen Y B, et al. 2020. Exploration of eco-environment and urbanization changes in coastal zones: A case study in China over the past 20 years. Ecological Indicators, 119: 106847, doi: 10.1016/j.ecolind.2020.106847.

Zheng Z H, Wu Z F, Chen Y B, et al. 2022. Instability of remote sensing based ecological index (RSEI) and its improvement for time series analysis. Science of The Total Environment, 814: 152595, doi: 10.1016/J.SCITOTENV.2021.152595.

Zhong L, Liu X S, Yang P. 2020. Regional development gap assessment method based on remote sensing images and weighted Theil index. Arabian Journal of Geosciences, 13(22): 1176, doi: 10.1007/s12517-020-06043-w.

Zhou J, Liu W. 2022. Monitoring and evaluation of eco-environment quality based on remote sensing-based ecological index (RSEI) in Taihu Lake Basin, China. Sustainability, 14(9): 5642, doi: 10.3390/su14095642.

Zhou Z Y, Wang X Q, Ding Z, et al. 2020. Remote sensing analysis of ecological quality change in Xinjiang. Acta Ecologica Sinica, 40(9): 2907–2919. (in Chinese)